

## Universal Gaussian basis sets for an optimum representation of Rydberg and continuum wavefunctions

This article has been downloaded from IOPscience. Please scroll down to see the full text article.

1989 J. Phys. B: At. Mol. Opt. Phys. 22 2223

(<http://iopscience.iop.org/0953-4075/22/14/007>)

View [the table of contents for this issue](#), or go to the [journal homepage](#) for more

Download details:

IP Address: 130.225.27.190

The article was downloaded on 01/04/2011 at 12:44

Please note that [terms and conditions apply](#).

# Universal Gaussian basis sets for an optimum representation of Rydberg and continuum wavefunctions

Karl Kaufmann, Werner Baumeister† and Martin Jungen

Institute of Physical Chemistry, University of Basel, Klingelbergstrasse 80, CH-4056 Basel, Switzerland

Received 22 March 1989

**Abstract.** A universal Gaussian basis set concept for the calculation of Rydberg and continuum states by pure  $L^2$  methods is presented. It is based on the generation of optimised sequences of Gaussian exponents by maximising the overlap with a series of Slater-type functions characterised by a constant exponent and a variable principal quantum number. In this way linear combinations of Gaussian basis functions can be found which are ideally suited to imitate Laguerre-Slater functions. It is thus possible to obtain optimum representations of Rydberg orbitals or of complete orthonormal systems of Laguerre functions playing an important role in the  $L^2$  expansion of continuum functions. The basis sets are tested with the hydrogen atom. The effectiveness of the basis is illustrated by the calculation of quantum defects associated with the s, p and d Rydberg series of the alkali metal atoms Li and Na. The phaseshifts determined in the ionisation continua of these systems nicely fit the series below the ionisation limit as is finally demonstrated by an Edlén plot.

## 1. Introduction

The accurate computation of energetically high-lying atomic or molecular Rydberg states by methods projecting the Hamiltonian into a space spanned by a finite set of square integrable functions requires a particularly careful choice of the basis set. The Rydberg functions which have to be represented cover a very large spatial domain and the radial part is characterised by a great number of nodes. Hence an expansion of Rydberg functions into nodeless Gaussian-type or Slater-type functions is extremely sensitive to improperly chosen basis functions. With inadequate basis sets only a few low-lying states can satisfactorily be described and for the higher members of the Rydberg series erroneous orbital energies result in wrong quantum defects. Because Slater-type functions show the correct asymptotic behaviour compared with bound hydrogen-like orbitals they were often used in *ab initio* calculations on Rydberg states (Bagus 1965, Snitchler and Watson 1986, Kundu and Mukherjee 1986). However, it has been demonstrated (Jungen 1981a) that Gaussians are equally well suited for this kind of calculation. But as a rule it is not sufficient to simply add a few diffuse basis functions to a Huzinaga (1965, 1969) basis which has been designed to optimally reproduce the cusp and the occupied shells of atoms in their ground state. It has been shown (Jungen 1981a) that it is essential to account for the nodal structure of the Rydberg orbitals.

† Present address: CIBA-GEIGY AG, CH-4002 Basel, Switzerland.

Therefore it is necessary to generate a corresponding sequence of Gaussian exponents by a suitable optimisation procedure. Such a procedure was suggested by Jungen (1981a) and with the resulting Gaussian basis sets a series of atomic and molecular Rydberg calculations have been successfully carried out (Staemmler *et al* 1981, Nager and Jungen 1982, Kaufmann *et al* 1983). Subsequently these basis sets have been refined by a numerical optimisation leading to further progress in Rydberg calculations (Kaufmann *et al* 1985, Cossart-Magos *et al* 1987, Jungen and Staemmler 1988). The new method presented in this work allows the generation of a sequence of Gaussians which yields more states of a Rydberg series and which entails less problems with linear dependence than the earlier method did.

Beyond the ionisation limit in the adjacent continuum similar problems arise in a much more severe form. Because Gaussian-type or Slater-type functions do not fulfil the asymptotic boundary conditions it seems nearly impossible to find representations of continuum functions with pure  $L^2$  methods. Even in a confined region around the origin the highly oscillatory behaviour of scattering solutions is very difficult to describe by a linear combination of nodeless square integrable functions. Therefore in most  $L^2$  methods additional functions are introduced which more efficiently simulate the oscillations of the continuum solutions. These augmented basis sets contain either numerically constructed functions (Nesbet *et al* 1984) or analytical functions such as Bessel (Lyons and Nesbet 1969, 1973) or harmonic oscillator functions (Kaufmann *et al* 1987) which are an extension of the simple Gaussians including a finite number of radial nodes. Another strategy to overcome these problems consists in doing the scattering calculation in a finite volume where the non-local interactions are strong and to span the scattering solutions only within this volume by a set of square integrable functions (Schneider 1975). Unfortunately these measures are accompanied by many additional technical labours often leading to a considerable increase in computation time. Therefore it would be of great interest to find Gaussian basis sets producing by the usual quantum chemical procedures eigensolutions in the continuum exhibiting the correct oscillatory behaviour in a limited region of space. This would have the distinct advantage of utilising the full power of existing molecular structure programs without being forced to rewrite a sophisticated integration code for some specially introduced basis functions.

The present work shows that this is indeed possible with the method already mentioned. Because of its general nature the procedure is able to generate sequences of Gaussian exponents which are designed to describe Rydberg functions or different sequences of basis functions which span low energy continuum solutions in a limited radial interval. The idea how this can be achieved and the underlying theory is outlined in §2. In §3 we derive a sequence of Gaussian exponents for describing Rydberg orbitals. The resulting basis is tested with the hydrogen atom and in order to illustrate the high quality of the basis it is applied in frozen-core calculations (Jungen 1981b) for the alkali atoms Li and Na. Section 4 is devoted to the generation of continuum basis sets and to the calculation of continuum solutions for the same systems. The Rydberg and continuum basis sets are discussed and compared with each other in the concluding section.

## 2. Theory

Our aim is to find a finite set of Gaussians which allows an optimum representation of either bound or continuum solutions of the Schrödinger equation for a hydrogen-like

system. The basis functions to be used take the following form

$$\chi_{lm}(\alpha, \mathbf{r}) = N_{\alpha l} r^l \exp(-\alpha r^2) Y_{lm}(\Omega_{\mathbf{r}}) \quad (1)$$

where the normalisation factor is given by

$$N_{\alpha l} = \left( \frac{2(2\alpha)^{l+3/2}}{\Gamma(l + \frac{3}{2})} \right)^{1/2}. \quad (2)$$

$Y_{lm}$  represents a surface spherical harmonic being a function of the space angle  $\Omega_{\mathbf{r}}$ . Equation (1) defines the so-called solid harmonic Gaussians from which real cartesian Gaussians orthogonal with respect to the angular coordinates can easily be constructed by appropriate linear combination. Generally the non-linear parameter  $\alpha$  characterises each individual basis function and is commonly designated as the exponent associated with the Gaussian function. For ground-state calculations it is chosen according to fixed rules, for example as prescribed by the even-tempered method (Raffenetti 1973, 1975). As explained in the introduction these rules have to be extended or replaced by new optimised series of exponents  $\{\alpha_i\}$  for the description of excited or continuum states. Because of the elaborate analytical structure of the hydrogen-like wavefunctions it does not seem very promising to search for a criterion which leads to a direct coherence between Gaussians and the solutions of the Schrödinger equation for a hydrogenic system. Instead we remember that there exists a complete orthonormal system of functions which spans the whole space of all discrete and continuum solutions. It was first introduced as a basis set into quantum chemistry by Shull and Loewdin (1955, 1959). The radial part of these functions is defined as follows

$$R_{nl}(r) = (2\zeta)^{3/2} \left( \frac{(n-l-1)!}{[(n+l+1)!]^3} \right)^{1/2} (2\zeta r)^l L_{n+l+1}^{2l+2}(2\zeta r) \exp(-\zeta r) \quad (3)$$

where  $L_{n+l+1}^{2l+2}$  represents an associated Laguerre polynomial of degree  $n-l-1$ . The scale factor  $\zeta$  is constant for all members of the set. For our purposes, it is a convenient property of the functions (3) that they can be formed by linear combination of Slater-type functions with constant exponent  $\zeta$ . This means that the optimisation problem can be reduced to an approximation problem of Slater functions by Gaussians. However, it is important to note in this context that in contrast to early optimisation procedures (Huzinaga 1965, 1969, Stewart 1969, 1970) we will *not* search for an expansion of Slater-type orbitals in terms of Gaussians. The central idea here is to approximate one Slater-type function characterised by the quantum number  $n$  by one Gaussian function characterised by the exponent  $\alpha$ . Performing the optimisation for a series of principal quantum numbers  $n$  thus generates a sequence  $\{\alpha_i\}$  ideally suited to imitate functions like (3) if applied as a basis set in quantum chemical calculations. For a Slater-type function we write

$$\chi_{nlm}(\zeta, \mathbf{r}) = N_{\zeta n} r^{n-1} \exp(-\zeta r) Y_{lm}(\Omega_{\mathbf{r}}) \quad (n = 1, 2, \dots) \quad (4)$$

with the normalisation factor

$$N_{\zeta n} = \frac{(2\zeta)^{n+1/2}}{[(2n)!]^{1/2}} \quad (5)$$

and where  $\zeta$  is held fixed. In order to obtain the best approximation we maximise the overlap between the functions (1) and (4) with respect to  $\alpha$ . After integrating over the angular coordinates we can formulate the overlap integral  $S$  as follows

$$S_{nl}(\alpha) = N_{\zeta n} N_{\alpha l} I_v(\alpha) \quad (0 < \alpha < \infty). \quad (6)$$

$I_v(\alpha)$  is the remaining integral over the radial coordinate

$$I_v(\alpha) = \int_0^\infty r^{v-1} \exp(-\zeta r) \exp(-\alpha r^2) dr \quad (7)$$

where  $v = n + l + 2$ . Equation (7) can be considered as the Laplace transform of a Gaussian function. Introducing the substitution

$$x = \zeta / 2\sqrt{\alpha} \quad (8)$$

and applying the transformation formula given by Erdélyi *et al* (1954) we find the following analytical expression for the radial integral

$$I_v(x) = \Gamma(v) 2^{v/2} (x/\zeta)^v \exp(x^2/2) D_{-v}(\sqrt{2}x). \quad (9)$$

Here  $D_{-v}$  denotes the parabolic cylinder function. For integer orders  $v = m$  the functions  $D_{-v}$  are related to the repeated integrals of the error function (Abramowitz and Stegun 1970)

$$D_{-m}(\sqrt{2}x) = (2^{(m-2)}\pi)^{1/2} \exp(x^2/2) i^{(m-1)} \operatorname{erfc}(x) \quad (10)$$

where

$$i^m \operatorname{erfc}(x) = \int_x^\infty i^{(m-1)} \operatorname{erfc}(t) dt \quad (m = 0, 1, 2, \dots) \quad (11)$$

and where  $\operatorname{erfc}(x)$  is the complementary error function

$$\operatorname{erfc}(x) = \frac{2}{\sqrt{\pi}} \int_x^\infty \exp(-t^2) dt.$$

Replacing  $D_{-v}$  in equation (9) by relation (10), including the product of normalisation factors and substituting  $v$  the overlap integral can be expressed in terms of the repeated integrals of the error function

$$S_{nl}(x) = A_{nl} x^{n+1/2} \exp(x^2) i^{(n+l+1)} \operatorname{erfc}(x) \quad (12)$$

where the prefactor  $A_{nl}$  is given by

$$A_{nl} = \left(\frac{1}{2}\pi\right)^{1/4} \frac{2^{(2n+l+2)}(n+l+1)!}{[(2n)!(2l+1)!]^{1/2}}.$$

For  $S_{nl}(x)$  to be a maximum with respect to  $x$  it is a necessary condition that the first derivative with respect to  $x$  vanishes. Due to the simple relationship (11) it is now very easy to obtain the derivative of  $S_{nl}(x)$ . Applying the well known three-term recurrence relations for  $i^m \operatorname{erfc}(x)$  (Abramowitz and Stegun 1970) to the derivative of

equation (12) we deduce after several algebraic manipulations the determining equation for a maximum overlap between the Slater-type function (4) and the Gaussian function (1)

$$2(n+l+2)(n+l+3)i^{(n+l+3)}\operatorname{erfc}(x_M) - (l+\frac{3}{2})i^{(n+l+1)}\operatorname{erfc}(x_M) = 0. \quad (13)$$

As can be shown by inspection of the functions  $i^m\operatorname{erfc}(x)$  (Abramowitz and Stegun 1970) equation (13) has one unique solution  $x_M$  which determines the maximum of  $S_{nl}(x)$  and therefore the optimum exponent  $\alpha$  via relation (8). From this point of view the numerical evaluation of  $x_M$  poses no special problems. However, care has to be taken in calculating the repeated integrals of the error function because with higher values of  $n$  and  $l$  one takes the risk of a rapid loss of accuracy of the computed  $x_M$  if the functions  $i^m\operatorname{erfc}(x)$  are not calculated with a sufficient number of significant digits. The reason for this is that the smoothly varying function represented by the left-hand side of equation (13) crosses the  $x$  axis with a nearly vanishing slope which makes the evaluation of  $x_M$  rather delicate. For the computation of  $i^m\operatorname{erfc}(x)$  we have therefore used a backward recurrence technique, as recommended by Gautschi (1961), combined with multiple precision arithmetic.

**Table 1.** Roots  $x_M(n, l)$  of equation (13).

$n$	$l = 0$	$l = 1$	$l = 2$	$l = 3$	$l = 4$
1	0.960 562				
2	1.571 619	1.191 941			
3	2.172 500	1.656 245	1.385 541		
4	2.767 292	2.116 982	1.774 249	1.555 352	
5	3.358 116	2.575 184	2.161 244	1.896 228	1.708 424
10	6.283 051	4.845 299	4.080 903	3.589 063	3.239 064
15	9.187 765	7.099 090	5.987 478	5.271 322	4.761 052
20	12.084 960	9.346 038	7.888 046	6.948 358	6.278 505

For the extremum search a safeguarded quadratic interpolation algorithm for univariate functions has been applied to the function  $1 - S_{nl}(x)$  and with the resulting values of  $x_M$  the residuals of equation (13) were calculated in order to check for accuracy. The calculations were done for all principal quantum numbers  $n$  ranging from  $n = 1$  to  $n = 20$  and the angular momenta  $l = 0, 1, 2, 3$  and  $4$ . For a few selected values of  $n$  and  $l$  the resulting roots  $x_M$  are collected in table 1. The values for the corresponding overlap integrals (12) are in the limits between 0.99 and 0.80.

The plot of all calculated values  $x_M$  against  $n$  in figure 1 reveals a remarkable relationship for the dependence of  $x_M$  on the quantum numbers  $n$  and  $l$ : it can excellently be approximated by a linear function for each  $l$ . A closer analytical examination of equation (13) shows that this is by no means obvious. However, it is quite reasonable if one takes into account that Slater-type orbitals have equidistant radial maxima, i.e.  $r_{\max} = (n-1)/\zeta$  and that the corresponding position for Gaussians is proportional to  $\alpha^{-1/2}$ . The results of a linear fit

$$x_M(n, l) \simeq a_l n + b_l \quad (14)$$

are tabulated together with the linear correlation coefficients  $\rho$  in table 2.

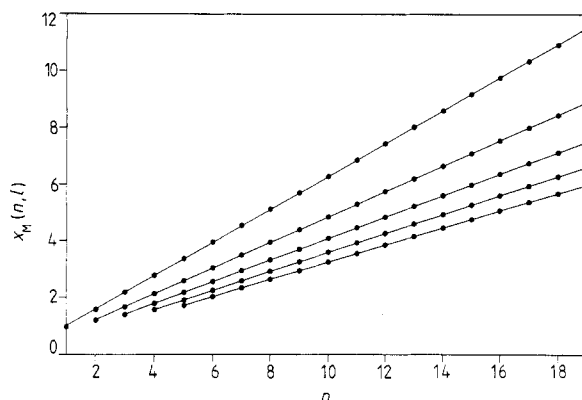


**Figure 1.** Dependence of the roots  $x_M(n, l)$  of equation (13) on the principal quantum number  $n$  for the angular momenta  $l = 0, 1, 2, 3$  and 4. For increasing angular momentum the slope of the straight lines is decreasing, i.e. the smallest slope corresponds to  $l = 4$ .

**Table 2.** Parameters  $a_l$  and  $b_l$  from a linear fit of  $x_M(n, l)$ .

	$l = 0$	$l = 1$	$l = 2$	$l = 3$	$l = 4$
$a_l$	0.584 342	0.452 615	0.382 362	0.337 027	0.304 679
$b_l$	0.424 483	0.309 805	0.251 333	0.215 013	0.189 944
$\rho$	0.999 986	0.999 992	0.999 996	0.999 998	0.999 998

The coefficients  $\rho$  really confirm that the function  $x_M(n, l)$  is extremely well described by the linear relation (14). Thus a very simple formula for the optimum Gaussian exponents  $\alpha$  is finally obtained

$$\alpha(n, l) = \left( \frac{\zeta}{2x_M(n, l)} \right)^2 \simeq \left( \frac{\zeta}{2(a_l n + b_l)} \right)^2. \quad (15)$$

This is the key equation of the present work. The formula will serve as a starting point for generating the optimum basis sequences  $\{\alpha_i\}$  in the following sections. Note that the linear approximation (14) offers the possibility to treat the quantum number  $n$  as a real parameter and to define basis functions for non-integer values of  $n$  as well which considerably increases the flexibility of the basis. Unfortunately the approximation process can not prevent the loss of the property of completeness characterising the original Slater basis (4) (Klahn and Bingel 1977). However, as will subsequently be shown the essential ability to reproduce the nodal structure of the wavefunctions in the outer spatial regions is fully conserved. Therefore it will only be necessary to extend the basis (15) to completeness if there is no inner-shell basis of the same symmetry at hand. For this purpose a few additional functions with higher exponents built according to the prescription proposed by Macías *et al* (1987) seem to be adequate.

### 3. Calculation of Rydberg states

Rydberg orbitals are closely related to the bound state solutions of a hydrogenic system.

The radial part of the latter functions has the form (Bethe and Salpeter 1957)

$$R_{nl}(r) = (2\zeta)^{3/2} \left( \frac{(n-l-1)!}{2n[(n+l)!]^3} \right)^{1/2} (2\zeta r)^l L_{n+l}^{2l+1}(2\zeta r) \exp(-\zeta r). \quad (16)$$

For a nuclear charge  $Z$  the scale factor is defined as  $\zeta = Z/n$ . With this definition of  $\zeta$  relation (15) for optimum Gaussian exponents becomes doubly indexed

$$\alpha_n(i, l) \simeq \left( \frac{Z}{2n} \right)^2 \frac{1}{(a_i l + b_l)^2} \quad (i = 1, 2, \dots, n) \quad (17)$$

where  $n = l + 1, \dots, \infty$  is the principal quantum number characterising a hydrogenic solution to be approximated. For the given index ranges equation (17) supplies the whole set of exponents  $\alpha$  which would be needed for an optimum representation of the first  $n - l$  functions (16) by linear combination of Gaussians. However, in a quantum chemical procedure where the linear combination coefficients of all basis functions are allowed to vary freely, a basis set like this would of course numerically be intractable. Because each basis function contributes to each solution it is sufficient to choose a suitable subset of basis functions from the whole basis set defined by equation (17). A glance at the functions (16) shows that the representation of the highly diffuse Rydberg orbitals in the asymptotic region is primarily determined by the Slater-type functions with the highest radial powers. It is therefore reasonable to select for a given principal quantum number  $n$  the exponents  $\alpha$  associated with indices  $i = n$  and  $i = n - 1$ . In this way those Gaussians which are best suited to reproduce the outermost loops of the Rydberg orbitals are automatically incorporated in the basis set. In order to eliminate one index from equation (17) we further simplify this expression by taking into account that the resulting products of the form  $n(n-1)$  appearing in the denominator of relation (17) for the specific choice  $i = n - 1$  can be approximated by  $(n - \frac{1}{2})^2$ . The consequence is that the final generation formula for the exponent sequences can be formulated as follows

$$\alpha(n, l) \simeq \left( \frac{Z}{2n} \right)^2 \frac{1}{(a_l n + b_l)^2} \quad (n = 1, \frac{3}{2}, 2, \frac{5}{2}, \dots). \quad (18)$$

Here the parameter  $Z$  is set equal to the net charge of the ionic core. Thus the corresponding exponents of the Rydberg basis are determined from equation (18) for every integer and half-integer value of  $n$ . The starting value of  $n$  is chosen in such a manner that the resulting exponent fits the inner-shell basis set describing the occupied core orbitals. The angular momentum dependent parameters  $a_l$  and  $b_l$  are taken from table 2. A similar discretisation procedure of  $\alpha$  space has already proved to be useful in earlier attempts with Rydberg calculations (Jungen 1981a).

The fundamental properties of Gaussian Rydberg basis sets relying on formula (18) shall be illustrated with three examples: H, Li and Na atoms. First a series of calculations on the hydrogen atom was performed in order to investigate the behaviour of the basis while increasing its size. The basis set used consists of a slightly modified Huzinaga (1965) 10s basis with exponents between 1170.5 and 0.044 allowing for a good description of the wavefunction near the nucleus and a Rydberg basis beginning with  $n = 2.0$  and ending with  $n = 5.0$ . The size of the Rydberg basis set has subsequently been enlarged up to  $n = 8.5$  with step size  $\Delta n = 0.5$  according to



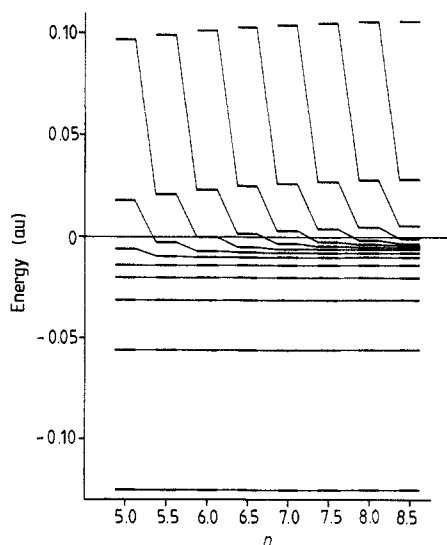


**Figure 2.** Dependence of the eigenvalue spectrum of the hydrogen atom on the size of the Gaussian Rydberg basis defined by equation (18).

equation (18). A limited portion of the eigenvalue spectrum of each calculation is depicted in figure 2. The diagram clearly demonstrates how the sequences of exponents resulting from application of equation (18) preferably stabilise the bound state solutions of a hydrogen-like system. On the average there appears one new eigenvalue below the ionisation limit with each new basis function added. Figure 3 shows a graph of a 10s hydrogenic radial function calculated with a Rydberg basis reaching up to  $n = 10.0$ . An excellent agreement with the analytical solution is achieved over the whole radial domain. The greatest absolute difference to the exact radial function is about  $5 \times 10^{-3}$  units. Note also that the exponential tail is reproduced with high accuracy.

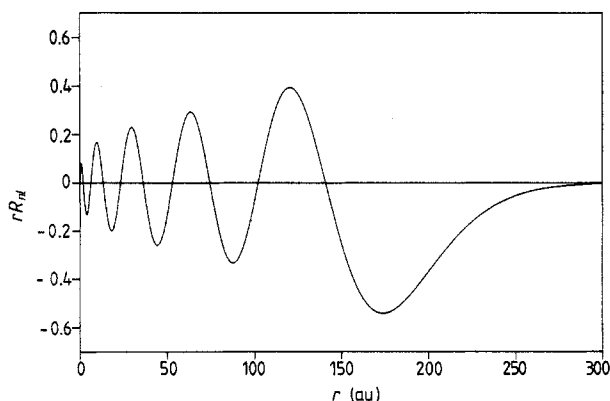


**Figure 3.** Hydrogenic radial function  $rR_{nl}(r)$  ( $n = 10$ ,  $l = 0$ ) calculated with a Gaussian Rydberg basis.

In the last years there has been a revival of interest in highly excited states due

to the introduction of tunable lasers allowing for a selective preparation of Rydberg atoms or molecules in states with definite quantum numbers. The classical prototypes for studying Rydberg states are alkali metal atoms. We have therefore decided to choose Li and Na as further testing examples for our basis sets. A quantity which is very sensitive to the quality of a calculated Rydberg orbital is the so called quantum defect  $\mu_l$  which depends on the orbital angular momentum  $l$  of the Rydberg electron. The orbital energies are approximately given by the famous Rydberg formula (Edlén 1964)

$$E_{nl} = -RZ_c^2(n - \mu_l)^{-2} \quad (19)$$

where  $R$  is the Rydberg constant and  $Z_c$  is the net charge of the ionic core. The denominator is often designated as the effective quantum number  $n_l^* = n - \mu_l$ . The quantum defect  $\mu_l$  accounts for the effective potential arising from the  $Z - 1$  core electrons and the nucleus of charge  $Z$  by shifting the energy eigenvalues away from the hydrogenic values. It shows a weak dependence on  $n$  being mainly determined by penetration and polarisation effects originating from the presence of the ionic core. In quantum defect theory  $\mu_l$  is defined as the asymptotic phaseshift  $\delta_l = \pi\mu_l$  of an exact atomic wavefunction relative to the corresponding Coulomb wavefunction (Seaton 1983).

We have calculated the quantum defects for s, p and d Rydberg series of the aforementioned alkali metal atoms. The computational procedure first consists in a conventional SCF calculation for the ions  $\text{Li}^+$  and  $\text{Na}^+$  with an appropriate cartesian Gaussian basis set. The basis is then augmented by diffuse functions whose exponents are defined by equation (18) allowing for the description of the Rydberg orbitals. The Rydberg states are calculated in the frozen-core approximation (Cohen and Kelly 1967, Jungen 1981b) using the SCF wavefunction of the ionic core. Consequently the interaction potential for the Rydberg electron with the core is a Hartree-Fock potential including full exchange but no polarisation. Hence the level of approximation is the same as in the so-called static-exchange methods. For the SCF calculation of  $\text{Li}^+$  a 13s Gaussian basis with exponents between 27 000 and 0.1012 is used according to Jungen (1981a). The SCF ground-state energy of the ion is then given by  $-7.236\,406$  au. The analogous calculation for  $\text{Na}^+$  with a [12s, 6p/12s, 4p] Gaussian basis (Veillard 1968) containing exponents in the range from 36 631.1 to 0.0246 yields an SCF energy of  $-161.670\,954$  au.

The basis used for evaluating the Rydberg states is specified in table 3 together with a few additional functions which have to be inserted in order to account for penetration and to guarantee a smooth adaptation of the Rydberg basis to the inner-shell basis. The Rydberg basis is designed to reproduce states up to a principal quantum number of at least  $n = 14$ . The maximum size of the total basis thus amounts to 43 functions for Li and 57 functions for Na. The resulting quantum defects  $\mu_l$  are collected in table 4 for Li and table 5 for Na, respectively. They are related to the orbital energies via relation (19).

It turns out that there is a very good agreement with the static-exchange values obtained from application of the Schwinger variational principle using a Slater basis (Watson 1983). Both tables show that the law of the series is obeyed up to the specified principal quantum number by the Rydberg basis set and hence really confirm the outstanding quality of the basis set. Note particularly that with  $n = 14$  a variation of the effective quantum number  $\Delta n_l^* = 1 \times 10^{-4}$  corresponds to an energy difference of

**Table 3.** Gaussian Rydberg basis for (a) lithium and (b) sodium. The last row specifies exponents according to equation (18). (For core basis see text.)

	$l = 0$	$l = 1$	$l = 2$
(a)			
	0.0495	24.000	1.5000
		6.0000	0.3750
		1.5000	0.1250
		0.5000	0.0587
		0.2205	0.0276
		0.0986	
	$n=2.0(0.5)12.0$	$n=2.0(0.5)13.0$	$n=3.0(0.5)14.0$
(b)			
	0.0111	0.1348	0.7320
		0.0422	0.1830
		0.0192	0.0609
			0.0276
	$n=3.0(0.5)12.0$	$n=3.0(0.5)13.0$	$n=3.0(0.5)14.0$

**Table 4.** Calculated and experimental quantum defects for lithium. Experimental values from Moore (1971).

	$l = 0$		$l = 1$		$l = 2$	
$n$	$\mu_{\text{calc}}$	$\mu_{\text{exp}}$	$\mu_{\text{calc}}$	$\mu_{\text{exp}}$	$\mu_{\text{calc}}$	$\mu_{\text{exp}}$
2	0.4071	0.4115	0.0285	0.0407		
3	0.3971	0.4039	0.0323	0.0445	0.0002	0.0015
4	0.3950	0.4018	0.0335	0.0457	0.0002	0.0017
5	0.3942	0.4009	0.0341	0.0463	0.0003	0.0018
6	0.3938	0.4004	0.0344	0.0470	0.0003	0.0018
7	0.3935	0.4004	0.0345	0.0472	0.0003	0.0021
8	0.3934	0.4007	0.0346	0.0487	0.0003	0.0032
9	0.3933	0.4008	0.0347	0.0470	0.0003	0.0040
10	0.3932	0.3942	0.0348	0.0486	0.0003	
11	0.3931		0.0348		0.0003	
12	0.3931		0.0349		0.0003	
13	0.3930		0.0349		0.0003	
14	0.3930		0.0350		0.0003	
15	0.3930					

less than  $0.1 \mu\text{Hartree}$ . The discrepancies between experiment and calculation originate from the neglect of electron correlation. The resulting errors of the quantum defect are practically constant for each Rydberg series. Thus the derivative of the quantum defect with respect to the energy, the slope of the so called Edlén plot, is correctly reproduced by our calculations as a variation of the quantum defect with respect to the principal quantum number. Within the method of calculation the quantum defects are accurate to  $1 \times 10^{-4}$  units. Finally we would like to point out that these computationally reproduced Rydberg series reaching up to the remarkably high quantum number of  $n = 15$  are obtained by a pure *ab initio* technique relying on the analytically simple nodeless Gaussian basis functions.

**Table 5.** Calculated and experimental quantum defects for sodium. Experimental values from Martin and Zalubas (1981).

<i>n</i>	<i>l</i> = 0		<i>l</i> = 1		<i>l</i> = 2	
	$\mu_{\text{calc}}$	$\mu_{\text{exp}}$	$\mu_{\text{calc}}$	$\mu_{\text{exp}}$	$\mu_{\text{calc}}$	$\mu_{\text{exp}}$
3	1.3405	1.3729	0.8621	0.8833	0.0028	0.0103
4	1.3283	1.3570	0.8473	0.8674	0.0038	0.0123
5	1.3246	1.3527	0.8422	0.8621	0.0044	0.0132
6	1.3230	1.3508	0.8399	0.8597	0.0046	0.0137
7	1.3222	1.3499	0.8386	0.8584	0.0048	0.0141
8	1.3217	1.3493	0.8378	0.8576	0.0049	0.0143
9	1.3214	1.3490	0.8373	0.8571	0.0050	0.0145
10	1.3212	1.3487	0.8370	0.8568	0.0051	0.0149
11	1.3211	1.3486	0.8367	0.8565	0.0051	0.0150
12	1.3210	1.3485	0.8365	0.8563	0.0052	0.0146
13	1.3209	1.3484	0.8364	0.8562	0.0052	0.0147
14	1.3208	1.3483	0.8363	0.8561	0.0052	0.0147
15	1.3208	1.3483	0.8362	0.8560	0.0052	0.0147
16	1.3208	1.3483				

#### 4. Calculation of continuum states

Since the early  $L^2$  basis set approaches for scattering calculations it is well known that explicit expansions of continuum Coulomb radial functions in special complete Laguerre–Slater basis sets can be found (Schwartz 1961, Yamani and Reinhardt 1975). The Slater exponent  $\zeta$  then plays the role of a scaling parameter which has the same value for all basis functions. The methods are primarily based on the particular property of these functions that the Schrödinger equation for a hydrogen-like system transforms into an analytically solvable three-term recurrence equation for the expansion coefficients. An imitation of such an  $L^2$  function space by Gaussians is possible if we directly refer to equation (15) of §2. The optimised sequence of Gaussian exponents is thus simply given by

$$\alpha(n, l) \simeq \frac{1}{4(a_l n + b_l)^2} \quad (n = 1, 2, \dots, N). \quad (20)$$

Because  $\zeta$  is related to the nuclear charge  $Z$  we define  $\zeta = 1$  according to the net ionic charge of the core seen by the scattering electron. In order to show the close relationship of a set of Gaussian-type functions with exponents relying on equation (20) to the corresponding Slater basis set we first look at a simple problem. Schwartz (1961) observed that the s-wave kinetic energy operator can be analytically diagonalised in a Laguerre–Slater basis. This means that the following discretisation of the continuous spectrum results if the basis is truncated after  $N$  functions

$$k_i = \frac{1}{2}\zeta \cot \left[ \frac{1}{2}\pi \left( 1 - \frac{i}{N+1} \right) \right] \quad (i = 1, 2, \dots, N) \quad (21)$$

where  $k_i$  is the wavenumber of the  $i$ th eigenvalue. Thus a finite matrix representation of the kinetic energy operator in the orthogonalised Gaussian basis set of dimension  $N$  should reproduce the eigenvalues (21) by diagonalisation. As is shown in table 6 this is indeed nicely fulfilled for the first few eigenvalues. The apparent regularity in

the low energy region clearly indicates that a spectrum similar to the sequence of levels in a spherical box is simulated by the Gaussian basis producing eigenfunctions with a sinusoidal behaviour inside the box. As is expected discrepancies only arise in the high energy part which does not bear any consequences concerning our purposes. By studying the eigenvalue spectrum of the attractive Coulomb Hamiltonian projected in this Gaussian basis we shall now demonstrate its suitability for continuum calculations. In the sequel we will present results obtained from calculations done in the ionisation continuum of the alkali metal atoms Li and Na.

**Table 6.** Discretisation of the s-wave kinetic energy operator in a Gaussian continuum basis of dimension  $N = 15$ .

$i$	Wavenumber $k_i$	
	Slater basis	Gaussian basis
1	0.0492	0.0487
2	0.0995	0.0979
3	0.1517	0.1480
4	0.2071	0.1994
5	0.2673	0.2528
6	0.3341	0.3090
7	0.4103	0.3691
8	0.5000	0.4342
9	0.6093	0.5065
10	0.7483	0.5888
11	0.9354	0.6857
12	1.2071	0.8052
13	1.6483	0.9622
14	2.5137	1.1906
15	5.0766	1.5935

With regard to a comparison with our Rydberg basis we have performed a similar series of calculations on the hydrogen atom using the Gaussian continuum basis generated from equation (20) for every integer  $n$  starting with  $n = 2$  and ending with  $n = 18$ . For the description of the inner part of the wavefunction the Huzinaga (1965) 10s basis again was employed where the two most diffuse functions were replaced by the first two members of the Gaussian continuum basis. The distribution of the resulting eigenvalues versus increasing dimension of the basis in the neighbourhood of the ionisation limit is graphically represented in figure 4. In contrast to figure 2 showing the analogous diagram for the Rydberg basis, it is evident from figure 4 that the eigenvalues produced with the current basis tend to accumulate in the continuous region of the hydrogenic spectrum. With each additional basis function the density of states above the ionisation limit is steadily increasing. We recognise that the bound states are also generated, but that more functions of type (20) than of type (18) are needed to reproduce the same number of bound states. This is a characteristic feature assigned to systems of square integrable functions spanning the whole space of discrete and continuum solutions of the Schrödinger equation. The mathematical relations between  $L^2$  eigenfunctions expanded in these special basis sets and the correct continuum solutions of the Schrödinger equation for a hydrogen-like system are comprised in the theory of equivalent quadrature developed and extensively discussed by Reinhardt (1979). Following his arguments we can consider our eigenfunctions

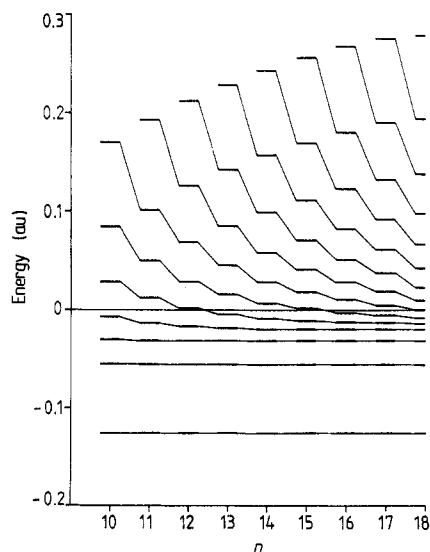


**Figure 4.** Dependence of the eigenvalue spectrum of the hydrogen atom on the size of the Gaussian continuum basis defined by equation (20).

belonging to positive energies as approximate projections on the hydrogenic continuum wavefunctions. Figure 5 impressively confirms this comprehension. It shows an  $L^2$  eigenfunction of the attractive Coulomb Hamiltonian compared with an exact radial Coulomb function for equal positive energy. Because the eigenfunction expanded in the Gaussian basis is not continuum normalised a normalisation factor has been computed by a fitting procedure involving the radial Coulomb function. The result is a surprisingly good coincidence of both functions persisting to a radius of approximately  $30 a_0$ . An excellent agreement is achieved at the points of inflection. However, it must be admitted that in the high energy region this relatively good quality of the radial function cannot be reached for numerical reasons. But with respect to our aims formulated in the introduction this is not of importance because we are primarily interested in the low energy region extending to about 0.2 au and below this limit all calculated eigenfunctions are of comparable quality to figure 5. At this point it is worthwhile emphasising that it is by no means obvious that an  $L^2$  eigenfunction with positive energy shows the desired oscillatory behaviour over a sufficiently large radial domain. If ordinary basis sets for bound-state calculations are used the eigenfunctions lying in the positive energy range rapidly collapse while probably showing unphysical, artificial features originating from basis set artifacts. Therefore a successful  $L^2$  calculation in the continuum heavily depends on the proper choice of the basis set.

The second part of figure 5 is devoted to a comparison of a selected member ( $n = 10, l = 0$ ) of the complete orthonormal system of Laguerre functions (3) with a linear combination of Gaussian functions. The coefficients of the Gaussians are determined by a linear least squares approximation procedure whereas the exponents are given by equation (20). In order to approximately reach completeness five additional functions with an exponent sequence according to Macías *et al* (1987) are used. The purpose of this graph is to demonstrate that our goal is evidently achieved of creating a Gaussian basis able to imitate the behaviour of these Laguerre–Slater functions playing

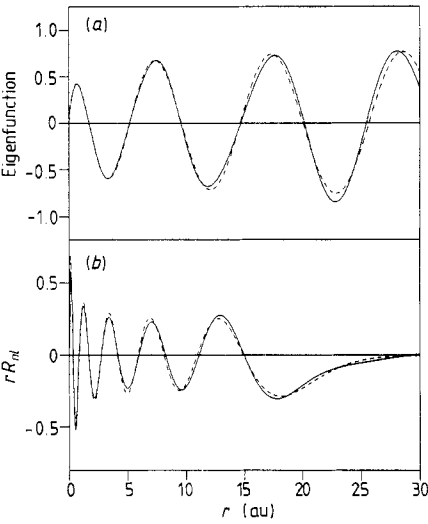


**Figure 5.** (a) Eigenfunction resulting from diagonalisation of a finite matrix representation of the attractive Coulomb Hamiltonian (full curve) compared with the exact radial Coulomb function ( $l = 0$ ,  $\varepsilon = 0.111\,806$  au). (b) Laguerre radial function  $rR_{nl}(r)$  ( $n = 10$ ,  $l = 0$ ) represented as a linear combination of Gaussian basis functions (full curve) compared with the exact function defined by equation (3). The additional exponents of the Gaussian functions are 9.625, 5.324, 2.758, 1.328, 0.589. The rest of the basis is given by  $n=1.0(1.0)10.0$  according to equation (20).

**Table 7.** Gaussian continuum basis for (a) lithium and (b) sodium. The last row specifies exponents according to equation (20). (For core basis see text.)

	$l = 0$	$l = 1$	$l = 2$
(a)			
		24.000	1.5000
		6.0000	0.3750
		1.5000	
		0.5000	
	$n=2.0(1.0)15.0$	$n=2.0(1.0)16.0$	$n=3.0(1.0)17.0$
(b)			
	0.2391	0.1689	0.6293
	0.0970		0.2437
	$n=3.0(1.0)15.0$	$n=3.0(1.0)16.0$	$n=3.0(1.0)17.0$

an important role in the finite  $L^2$  basis expansion of continuum wavefunctions.

In order to provide a quantitative measure of the effectiveness of our Gaussian continuum basis we finally present quantum defects  $\mu_l$  calculated in the ionisation continuum of Li and Na. The method of calculation has been described in great detail by Kaufmann *et al* (1987) and will only be summarised here. Briefly the procedure is based on the generation of a tridiagonal matrix representation via the Lanczos algorithm (Lanczos 1950) of an effective one-electron Hamiltonian, i.e. of the frozen-core operator (Jungen 1981b). This allows for the recursive construction of a

wavefunction at a selected energy yielding an  $L^2$  approximation of the corresponding continuum solution. Concerning this aspect the method is related to the analytical  $J$ -matrix techniques (Heller and Yamani 1974). We therefore expect our Gaussian basis, which has been designed to optimally reproduce Laguerre–Slater functions, to be particularly suited for this kind of  $L^2$  basis set approach in the continuum. The phaseshift  $\delta_l$  due to the non-Coulomb field in the inner core can be deduced from the coefficients in a superposition of a regular and irregular Coulomb function fitted to the computed radial function outside the core. The basis sets used in these calculations are specified in table 7. The basis sets to describe the ionic closed-shell cores  $\text{Li}^+$  and  $\text{Na}^+$  are identical to those used in the Rydberg calculations.

**Table 8.** Quantum defects calculated in the ionisation continuum of lithium.

Energy (au)	Quantum defects $\mu_l$		
	$l = 0$	$l = 1$	$l = 2$
0.00	0.3929	0.0353	0.0007
0.05	0.3896	0.0373	0.0013
0.10	0.3868	0.0391	0.0011
0.15	0.3845	0.0404	0.0007
0.20	0.3814	0.0445	−0.0005

**Table 9.** Quantum defects calculated in the ionisation continuum of sodium.

Energy (au)	Quantum defects $\mu_l$		
	$l = 0$	$l = 1$	$l = 2$
0.00	1.3217	0.8361	0.0053
0.05	1.3163	0.8258	0.0066
0.10	1.3127	0.8154	0.0107
0.15	1.3048	0.8063	0.0111
0.20	1.3021	0.7961	0.0204

The quantum defects  $\mu_l = \delta_l/\pi$  computed at equidistant energies between 0 and 0.2 au are collected in tables 8 and 9 for Li and Na respectively. The radial interval used for the determination of the phaseshifts  $\delta_l$  extends from  $2a_0$  to  $15a_0$ . The absolute accuracy of the calculated quantum defects  $\mu_l$  in the ionisation continuum is about one order of magnitude less than in the discrete spectrum, i.e.  $1 \times 10^{-3}$ . Nevertheless as is required by quantum defect theory (Seaton 1983) the quantum defects  $\mu_l$  determined from the  $L^2$  wavefunctions above the ionisation limit fit excellently the series calculated in the previous section below the ionisation limit. With respect to a comparison with our previous work in which we have employed harmonic oscillator functions in the basis we complete this section with a graphical representation of one radial function used to extract the associated quantum defect for each system. Figure 6, together with the tabulated quantum defects, clearly proves that at least for low energy scattering properly chosen Gaussian basis functions are thoroughly able to simulate the oscillations of the continuum solutions.



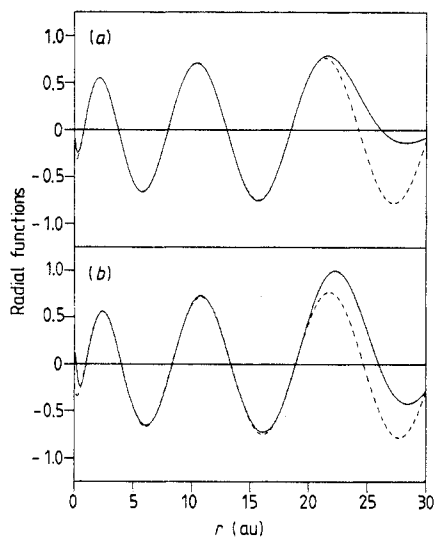


**Figure 6.** Phaseshifted continuum radial functions of: (a) lithium and (b) sodium with  $l = 0$  and  $\varepsilon = 0.1$  au. Quantum-chemical calculations (full curves) are compared with exact numerical Coulomb functions.

## 5. Conclusions

We have presented a basis set concept for pure  $L^2$  Rydberg and continuum calculations. It is based on the idea of generating a Gaussian basis by approximating in the least-squares sense a set of Slater-type functions which constitute a basis for Laguerre–Slater functions forming on their part either eigenfunctions (16) of the Coulomb Hamiltonian or a complete orthonormal set like the functions (3). The above obtained results of the Rydberg and continuum calculations relying on these basis sets are commonly represented in a Edlén plot (Edlén 1964) for s and p series. From figure 7 it turns out that the calculated quantum defects characterising the Rydberg series directly pass into the phaseshifts in the ionisation continuum as it should be according to the fundamental requirement of quantum defect theory (Seaton 1983)

$$\lim_{n \rightarrow \infty} \pi \mu_l = \lim_{E \rightarrow 0} \delta_l. \quad (22)$$

We note that these results were produced with a single basis for each angular momentum quantum number. In this way full advantage could be taken of a basis set method to treat an entire Rydberg series simultaneously. Due to the universal applicability of relation (15) we could even use the same  $l$ -Rydberg or  $l$ -continuum basis functions for different atomic systems. Only the transition from the inner-shell basis determined by the physical nature of the ionic core to the outer basis has to be smoothed out individually. Application of these basis sets to molecular systems is straightforward if placed in the centre of mass or the centre of charge. Although different basis sets were used for the Rydberg and continuum parts, they have a common origin in the parametrised formula (15). The parameter  $\zeta$  can be used to influence the extension of the basis in configuration space while  $n$  fixes the extension of function space. This means that the upper limit of a Rydberg series can be predicted up to which reliable results are obtainable by the calculation or that the optimum expansion length

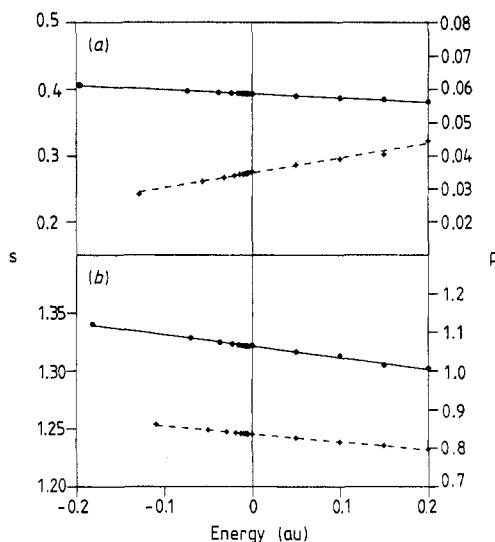


**Figure 7.** Edlén plots of the calculated quantum defects in the s (full curves) and p (broken curves) Rydberg series and ionisation continua respectively of (a) lithium and (b) sodium.

of the continuum orbitals in terms of Lanczos functions can be estimated. However, for numerical reasons the basis sets can not be arbitrarily enlarged. Experience shows that the practical limit is given by values of  $n$  lying between 15 and 20, which is sufficient for most applications. Beyond these limits the linear dependence of the basis gets dramatically worse giving rise to numerically unstable solutions in the calculation or preventing any calculation in finite arithmetic at all. But it is important to point out that this is *not* a deficiency of the basis. The phenomenon of near-linear dependence is inherent in the nature of the problem, which is to represent highly oscillatory functions as linear combinations of nodeless square integrable functions. This difficulty can be efficiently tackled by carefully programming stable algorithms and exploiting multiple precision arithmetic which is available in most today's computer architectures. The actual calculations have been performed in double precision arithmetic (16 decimal digits) throughout thus proving that these problems can be successfully treated.

A final survey over the numerical results in this work leads us to the conclusion that we would expect our Gaussian continuum basis to be especially suited for application in several existing numerical  $L^2$  basis set approaches frequently used in the last years to handle electronic continua. As a few representatives we mention stabilisation procedures (Hazi and Taylor 1970), Stieltjes moment calculations (Reinhardt 1979) or Feshbach projection techniques (Feshbach 1958, 1962). Concerning the significance which is associated with the system of functions (3) not only for the expansion of continuum wavefunctions but also in connection with the treatment of interelectronic correlation (Shull and Loewdin 1955, 1959) a further investigation of the behaviour of these optimised Gaussian functions in quantum chemical procedures seems to be very promising. Hence the work presented in this paper can be considered as an attempt to endow  $L^2$  basis set methods for Rydberg and continuum calculations with basis functions as efficient and simple to use as those employed for a long time by conventional atomic and molecular ground-state calculation methods.

## Acknowledgments

This work is part of project 2.461-0.87 of the Schweizerischer Nationalfonds and has been supported by the CIBA-Stiftung (Basel).

## References

- Abramowitz M and Stegun I 1970 *Handbook of Mathematical Functions* (New York: Dover)
- Bagus R 1965 *Phys. Rev.* **139** 619
- Bethe H A and Salpeter E E 1957 *Handbuch der Physik* vol 35 (Berlin: Springer)
- Cohen M and Kelly P S 1967 *Can. J. Phys.* **45** 1661
- Cossart-Magos C, Jungen M and Launay F 1987 *Mol. Phys.* **61** 1077
- Edlén B 1964 *Handbuch der Physik* vol 27 (Berlin: Springer)
- Erdélyi A, Magnus W, Oberhettinger F and Tricomi F G 1954 *Tables of Integral Transforms* vol 2 (New York: McGraw-Hill)
- Feshbach H 1958 *Ann. Phys., NY* **5** 357
- 1962 *Ann. Phys., NY* **19** 287
- Gautschi W 1961 *Math. Comput.* **15** 227
- Hazi A U and Taylor H S 1970 *Phys. Rev. A* **1** 1109
- Heller E J and Yamani H A 1974 *Phys. Rev. A* **9** 1201
- Huzinaga S 1965 *J. Chem. Phys.* **42** 1293
- 1969 *J. Chem. Phys.* **50** 1371
- Jungen M 1981a *J. Chem. Phys.* **74** 750
- 1981b *Theor. Chim. Acta* **60** 369
- Jungen M and Staemmler V 1988 *J. Phys. B: At. Mol. Opt. Phys.* **21** 463
- Kaufmann K, Baumeister W and Jungen M 1987 *J. Phys. B: At. Mol. Phys.* **20** 4299
- Kaufmann K, Jungen M and Staemmler V 1983 *Chem. Phys.* **79** 111
- Kaufmann K, Nager Ch and Jungen M 1985 *Chem. Phys.* **95** 385
- Klahn B and Bingel W A 1977 *Theor. Chim. Acta* **44** 27
- Kundu B and Mukherjee P K 1986 *Theor. Chim. Acta* **69** 51
- Lanczos C 1950 *J. Res. NBS* **45** 917
- Lyons J D and Nesbet R K 1969 *J. Comput. Phys.* **4** 499
- 1973 *J. Comput. Phys.* **11** 166
- Macías A, Martín F, Riera A and Yáñez 1987 *Phys. Rev. A* **36** 4179
- Martin W C and Zalubas R 1981 *J. Phys. Chem. Ref. Data* **10** 153
- Moore C E 1971 *Atomic Energy Levels* (Nat. Standard Reference Data Series No 35) p 8
- Nager Ch and Jungen M 1982 *Chem. Phys.* **70** 189
- Nesbet R K, Noble C J, Morgan L A and Weatherford 1984 *J. Phys. B: At. Mol. Phys.* **17** L891
- Raffenetti R C 1973 *J. Chem. Phys.* **59** 5936
- 1975 *Int. J. Quantum Chem.* **9** 289
- Reinhardt W P 1979 *Comput. Phys. Commun.* **17** 1
- Schneider B 1975 *Chem. Phys. Lett.* **31** 237
- Schwarz C 1961 *Ann. Phys., NY* **16** 36
- Seaton M J 1983 *Rep. Prog. Phys.* **46** 167
- Shull H and Loewdin P O 1955 *J. Chem. Phys.* **23** 1362
- 1959 *J. Chem. Phys.* **30** 617
- Snitchler G L and Watson D K 1986 *J. Phys. B: At. Mol. Phys.* **19** 259
- Staemmler V, Jaquet R and Jungen M 1981 *J. Chem. Phys.* **74** 1285
- Stewart R F 1969 *J. Chem. Phys.* **50** 2485
- 1970 *J. Chem. Phys.* **52** 431
- Veillard A 1968 *Theor. Chim. Acta* **12** 405
- Watson D K 1983 *Phys. Rev. A* **28** 40
- Yamani H A and Reinhardt W P 1975 *Phys. Rev. A* **11** 1144